



# Tumor-like features of gene expression and metabolic profiles in enlarged pancreatic islets are associated with impaired incretin-induced insulin secretion in obese diabetes: A...

Hayami, Tomohide ; Yokoi, Norihide ; Yamaguchi, Takuro ; Honda, Kohei ; Murao, Naoya ; Takahashi, Harumi ; Wang, Shujie ; Seino, Yusuke ;...

---

(Citation)

Journal of Diabetes Investigation, 11(6):1434-1447

(Issue Date)

2020-11

(Resource Type)

journal article

(Version)

Version of Record

(Rights)

© 2020 The Authors. Journal of Diabetes Investigation published by Asian Association for the Study of Diabetes (AASD) and John Wiley & Sons Australia, Ltd.






This is an open access article under the terms of the Creative Commons Attribution - NonCommercial - NoDerivs License, which permits use and distribution in any medium,...

(URL)

<https://hdl.handle.net/20.500.14094/90007584>



# Tumor-like features of gene expression and metabolic profiles in enlarged pancreatic islets are associated with impaired incretin-induced insulin secretion in obese diabetes: A study of Zucker fatty diabetes mellitus rat

Tomohide Hayami<sup>1,2,3</sup> , Norihide Yokoi<sup>1,2,\*</sup> , Takuro Yamaguchi<sup>1,2</sup>, Kohei Honda<sup>1</sup>, Naoya Murao<sup>1</sup>, Harumi Takahashi<sup>1,2</sup>, Shujie Wang<sup>4</sup>, Yusuke Seino<sup>5</sup> , Hideki Kamiya<sup>3</sup>, Daisuke Yabe<sup>1,2,\*</sup> , Ian R Sweet<sup>6</sup>, Akira Mizoguchi<sup>4</sup>, Jiro Nakamura<sup>3</sup>, Susumu Seino<sup>1,2,\*</sup> 

<sup>1</sup>Division of Molecular and Metabolic Medicine, Department of Physiology and Cell Biology, Kobe University Graduate School of Medicine, Kobe, Japan, <sup>2</sup>Kansai Electric Power Medical Research Institute, Kobe, Japan, <sup>3</sup>Division of Diabetes, Department of Internal Medicine, Aichi Medical University, Nagakute, Japan, <sup>4</sup>Department of Neural Regeneration and Cell Communication, Mie University Graduate School of Medicine, Tsu, Japan, <sup>5</sup>Division of Endocrinology and Metabolism, Department of Internal Medicine, Fujita Health University, Toyoake, Japan, and <sup>6</sup>Department of Medicine, Division of Metabolism, Endocrinology and Nutrition, University of Washington, Seattle, Washington, USA

## Keywords

Enlarged islets, Incretin, Tumor cells

## \*Correspondence

Norihide Yokoi or Susumu Seino  
Tel.: +81-78-304-6061  
Fax: +81-78-304-6064  
E-mail address:  
yokoi.norihide.5w@kyoto-u.ac.jp or  
seino@med.kobe-u.ac.jp

*J Diabetes Investig* 2020; 11: 1434–1447

doi:10.1111/jdi.13272

## ABSTRACT

**Aims/Introduction:** Pancreatic islets are heterogenous. To clarify the relationship between islet heterogeneity and incretin action in the islets, we studied gene expression and metabolic profiles of non-large and enlarged islets of the Zucker fatty diabetes mellitus rat, an obese diabetes model, as well as incretin-induced insulin secretion (IIS) in these islets.

**Materials and Methods:** Pancreatic islets of control (*fa/+*) and fatty (*fa/fa*) rats at 8 and 12 weeks-of-age were isolated. The islets of *fa/fa* rats at 12 weeks-of-age were separated into non-large islets ( $\leq 200$   $\mu\text{m}$  in diameter) and enlarged islets ( $> 300$   $\mu\text{m}$  in diameter). Morphological analyses, insulin secretion experiments, transcriptome analysis, metabolome analysis and oxygen consumption analysis were carried out on these islets.

**Results:** The number of enlarged islets was increased with age in fatty rats, and IIS was significantly reduced in the enlarged islets. Markers for  $\beta$ -cell differentiation were markedly decreased in the enlarged islets, but those for cell proliferation were increased. Glycolysis was enhanced in the enlarged islets, whereas the tricarboxylic acid cycle was suppressed. The oxygen consumption rate under glucose stimulation was reduced in the enlarged islets. Production of glutamate, a key signal for IIS, was decreased in the enlarged islets.

**Conclusions:** The enlarged islets of Zucker fatty diabetes mellitus rats, which are defective for IIS, show tumor cell-like metabolic features, including a dedifferentiated state, accelerated aerobic glycolysis and impaired mitochondrial function. The age-dependent increase in such islets could contribute to the pathophysiology of obese diabetes.

<sup>†</sup>Present address: Laboratory of Animal Breeding and Genetics, Division of Applied Biosciences, Kyoto University Graduate School of Agriculture, Kitashirakawa Oiwake-cho, Sakyo-ku, Kyoto, Japan.

<sup>‡</sup>Present address: Department of Diabetes and Endocrinology, Gifu University Graduate School of Medicine, Gifu, Japan.

Received 23 October 2019; revised 26 March 2020; accepted 5 April 2020

## INTRODUCTION

Pancreatic  $\beta$ -cells play a central role in the regulation of blood glucose level by secreting insulin. Dysregulation of insulin secretion contributes to the development of diabetes, obesity and hypoglycemia. Glucose is the essential fuel that regulates insulin

secretion. In addition to glucose-induced insulin secretion (GIIS), neuronal and hormonal inputs are also required for normal regulation of insulin secretion. The “incretin” gut hormones, glucagon-like peptide 1 (GLP-1) and glucose-dependent insulinotropic polypeptide (GIP), which are secreted from enteroendocrine cells in response to meal ingestion, potentiate insulin secretion in a glucose-dependent manner primarily through cyclic adenosine monophosphate signaling in the  $\beta$ -cells<sup>1</sup>. It has been shown that sensitivities of the  $\beta$ -cells to endogenous incretins and exogenously administered incretins or incretin-based antidiabetic drugs are reduced in type 2 diabetes and obesity<sup>2–4</sup>. We previously found that glutamate produced by glucose through the malate-aspartate (MA) shuttle in the  $\beta$ -cells links glucose metabolism to cyclic adenosine monophosphate action in insulin granule exocytosis, and is a critical cell signal in incretin-induced insulin secretion (IIIS)<sup>5,6</sup>. We also showed that impaired glutamate production in the pancreatic islets is well correlated with impairment of IIIS in animal models of diabetes (Goto-Kakizaki rat) and obesity (Zucker fatty rat)<sup>5</sup>.

Pancreatic islets are morphologically and functionally heterogeneous<sup>7,8</sup>. It has been shown that smaller islets generally retain more insulin secretory capacity compared with larger islets<sup>9,10</sup>, and that smaller islets comprise more  $\beta$ -cells with higher insulin content than larger islets<sup>11</sup>. It has also been reported that there is a preferential loss of larger islets ( $>60\ \mu\text{m}$  in diameter) in type 2 diabetes patients compared with non-diabetic individuals<sup>12</sup>. Furthermore, the distribution of small and large pancreatic islets might change in the course of the development of diabetes and obesity, which could contribute to the pathogenesis and pathophysiology of the disease. However, the relationship between size and function of pancreatic islets in the diabetic state remains to be determined. The Zucker fatty diabetes mellitus (ZFDM) rat has recently been established as an animal model of obese type 2 diabetes<sup>13</sup>. The ZFDM rat originated from the obese ZF rat, and harbors a missense mutation (*fatty*, referred to as *fa*) in the leptin receptor gene. We found that IIIS from pancreatic islets of ZFDM *fa/fa* rats is diminished at 11 weeks-of-age<sup>14</sup>, and that their pancreata contain both non-large and enlarged islets. Thus, the ZFDM rat is a useful model for investigating morphological and functional heterogeneity of islets, as well as incretin unresponsiveness in obese type 2 diabetes.

In the present study, we studied islets of control lean *fa/+* rats and non-large islets (defined as  $\leq 200\ \mu\text{m}$  in diameter) and enlarged islets (defined as  $>300\ \mu\text{m}$  in diameter) of *fa/fa* rats of the ZFDM strain separately, to clarify the mechanism underlying functional differences between non-large islets and enlarged islets. We found that enlarged pancreatic islets show tumor cell-like metabolic features of glucose metabolism accompanied with reduced glutamate production. Such metabolic changes could contribute to the development of incretin unresponsiveness in obese diabetes.

## METHODS

### Animals

Male ZFDM rats (Hos:ZFDM-*Lepr*<sup>*fa/fa*</sup> and Hos:ZFDM-*Lepr*<sup>*fa/+*</sup>) were provided by Hoshino Laboratory Animals, Inc. (Ibaraki, Japan). All animals were maintained under specific pathogen-free conditions with a 12-h light–dark cycle, and were provided with a commercial diet CE-2 (CLEA Japan, Inc., Tokyo, Japan) at the Animal Facility of Kobe Biotechnology Research and Human Resource Development Center of Kobe University. At the end of the experiments, animals were killed by an overdose of anesthetic with pentobarbital sodium. All animal experiments were approved by the Committee on Animal Experimentation of Kobe University, and carried out in accordance with the Guidelines for Animal Experimentation at Kobe University.

### Oral glucose tolerance test and intravenous glucose tolerance test

The oral glucose tolerance test was carried out as described previously<sup>14</sup>. In brief, glucose (2.0 g/kg bodyweight) was administered orally to 6-h fasted rats, and blood samples were collected from the tail vein at indicated time points. The intravenous glucose tolerance test was carried out as described previously<sup>15</sup>. In brief, glucose (1.0 g/kg bodyweight) was administered into the jugular vein of 16-h fasted rats after anesthesia by intraperitoneal injection of pentobarbital sodium and subcutaneous injection of ketoprofen, and blood samples were taken from the femoral vein at indicated time points. Blood glucose levels were measured by a portable glucose meter (ANTSENSE III, HORIBA, Ltd., Kyoto, Japan). Plasma GLP-1 and GIP levels were measured by total GLP-1 kit (version 2; Meso Scale Diagnostics, Rockville, MD, USA) and Rat/Mouse total GIP ELISA kit (Millipore, Billerica, MA, USA), respectively.

### Isolation of the pancreatic islets

Pancreatic islets were isolated by the collagenase digestion and Ficoll gradient method<sup>16,17</sup>. Isolated pancreatic islets were cultured for 3 days in RPMI1640 (Sigma-Aldrich, St. Louis, MO, USA) before experiments.

### Insulin secretion experiment

Insulin secretion experiments were carried out as described previously<sup>14</sup>.

### Immunohistochemistry

Immunohistochemistry was carried out as described previously<sup>18</sup>. Primary antibodies were: guinea pig polyclonal anti-insulin (ab7842; Abcam, Tokyo, Japan; 1:100), mouse monoclonal anti-glucagon (G2654, Dako Japan, Tokyo, Japan; 1:2,000), rabbit monoclonal anti-Glp1r (ab218532; Abcam; 1:500), rabbit polyclonal anti-Pdx1 (5796; Cell Signaling Technology, Tokyo, Japan; 1:400), rabbit monoclonal anti-Myc (10828-1-AP; Proteintech Japan, Tokyo, Japan; 1:50) and rabbit monoclonal

anti-Ki67 (9129; Cell Signaling Technology, Tokyo, Japan; 1:400). The  $\beta$ -cell area was detected by insulin staining, and the number of  $\beta$ -cells was detected by 4',6-diamidino-2-phenylindole staining. The size of the  $\beta$ -cells in each islet was calculated by the formula "total  $\beta$ -cell area divided by number of  $\beta$ -cells" (50 islets of 3–4 rats for each genotype). The  $\alpha$ -cell area was detected by glucagon staining, and ratio of the  $\alpha$ - or  $\beta$ -cell area in the whole pancreas was calculated by the formula "total  $\alpha$ - or  $\beta$ -cell area divided by whole pancreas area" (6–9 pancreas sections of 3–4 rats for each genotype).

### Ribonucleic acid sequencing

Ribonucleic acid (RNA) sequencing was carried out on 1  $\mu$ g each of total RNA, using an Illumina HiSeq 2500 system by Eurofins Genomics (Ebersberg, Germany). Sequence reads were cleaned using Trimmomatic (version 0.32), and then aligned to the mouse genome (GRCm38) using Bowtie (version 2-2.2.2) and TopHat (version 2.0.11). Raw read counts and fragments per kilobase of transcript per million mapped reads were generated using Cufflinks (version 2.2.1). Transcripts were merged using Cuffmerge (version 2.2.1) and differential gene expression was determined using Cuffdiff (version 2.2.1). The RNA sequencing data have been deposited in DDBJ Sequence Read Archive (DRA) with the accession number DRA007109 and DRA007371.

### Pathway analysis

Pathway analysis of differentially expressed genes among islets of *fa/+* and *fa/fa* rats at 12 weeks-of-age (nominal  $P < 0.05$  and fold change  $> 1.5$ ) was carried out by using the Functional Annotation Tool of the DAVID Bioinformatics Resources 6.8.<sup>19,20</sup>

### Metabolome analysis

Pancreatic islets were pre-incubated for 30 min in HEPES-balanced Krebs-Ringer bicarbonate buffer containing 0.1% bovine serum albumin (H-KRB) with 2.8 mmol/L glucose, and then incubated for 30 min in H-KRB with 2.8 mmol/L or 11.2 mmol/L glucose. Extraction and quantification of hydrophilic metabolites were carried out as described previously.<sup>5</sup> The contents of metabolites were normalized by the cellular protein content.

### Lactate measurement

Pancreatic islets were cultured in RPMI containing 11.1 mmol/L glucose for 20 h. The culture medium was corrected, and lactate in the medium was measured by Lactate Assay Kit-WST (Fujifilm Wako, Osaka, Japan). The amount of lactate was corrected by the amount of protein in the pancreatic islets used for the culture.

### Transmission electron microscopy

Transmission electron microscopy was carried out as described previously.<sup>21</sup>

### Oxygen consumption rate

The oxygen consumption rate (OCR) was measured as described previously.<sup>22</sup>

### Statistical analysis

Data are expressed as the mean  $\pm$  standard error of the mean. Differences among the groups were analyzed with Holm's method (also known as sequentially rejective Bonferroni test) or Welch's *t*-test, as indicated in the figure legends.  $P < 0.05$  was regarded as statistically significant.

## RESULTS

### Glucose tolerance to oral but not intravenous load is deteriorated with age in ZFDM *fa/fa* rats, without a defect in incretin secretion

Glucose tolerance to oral load was deteriorated markedly in *fa/fa* rats at 12 weeks-of-age (Figure 1a). In contrast, glucose tolerance to intravenous load was not changed with age (Figure 1b). During the oral glucose tolerance test, both plasma GLP-1 and GIP levels of *fa/fa* rats were higher than those of *fa/+* rats, and there was no difference in GLP-1 and GIP levels of *fa/fa* rats between 8 and 12 weeks-of-age (Figure 1c,d). These results show that incretin responsiveness, but not incretin secretion, is deteriorated with age in ZFDM *fa/fa* rats.

### Pancreata of ZFDM *fa/fa* rats at 12 weeks-of-age contain both non-large and enlarged islets

Microscopic examination of isolated islets showed that a majority of islets of control *fa/+* rats were normal in size ( $\leq 200$   $\mu$ m in diameter) at both 8 weeks and 12 weeks-of-age (Figure 2a). In ZFDM *fa/fa* rats, although the size of pancreatic islets was normal or slightly larger at 8 weeks-of-age, a significant portion of the islets showed diameter  $> 300$   $\mu$ m at 12 weeks-of-age. We then determined the size distribution of the islets by measuring diameters under microscopy, and found that islets exceeding 300  $\mu$ m in diameter (enlarged islets) were present specifically in *fa/fa* rats, whereas a majority of the islets of *fa/+* rats were  $\leq 200$   $\mu$ m in diameter (non-large islets; Figure 2b, Figure S1a). Although the number of enlarged islets occupied  $\sim 10\%$  of total islet number at 12 weeks-of-age, the estimated volume of enlarged islets occupied  $\sim 60\%$  of total islet volume (Figure S1b). We also found that the sizes of the islets were widely distributed in *fa/fa* rats at 12 weeks-of-age, and that the number of enlarged islets in *fa/fa* rats was increased, compared with that at 8 weeks-of-age. A majority of the enlarged islets at 12 weeks-of-age showed irregular shapes, but generally retained the architecture (Figure 2c). As the enlarged islets comprised mainly insulin-positive cells with glucagon-positive cells at the periphery (Figure 2c), the majority of the islets examined in this study were likely to be  $\beta$ -cells. The ratio of  $\beta$ -cell area in the whole pancreas was not changed at 8 and 12 weeks in both *fa/+* and *fa/fa* rats, whereas that of  $\alpha$ -cell area was decreased at 12 weeks-of-age (Figure S2). In addition, the individual  $\beta$ -cell size of *fa/fa* rats was not enlarged, but was similar to that of

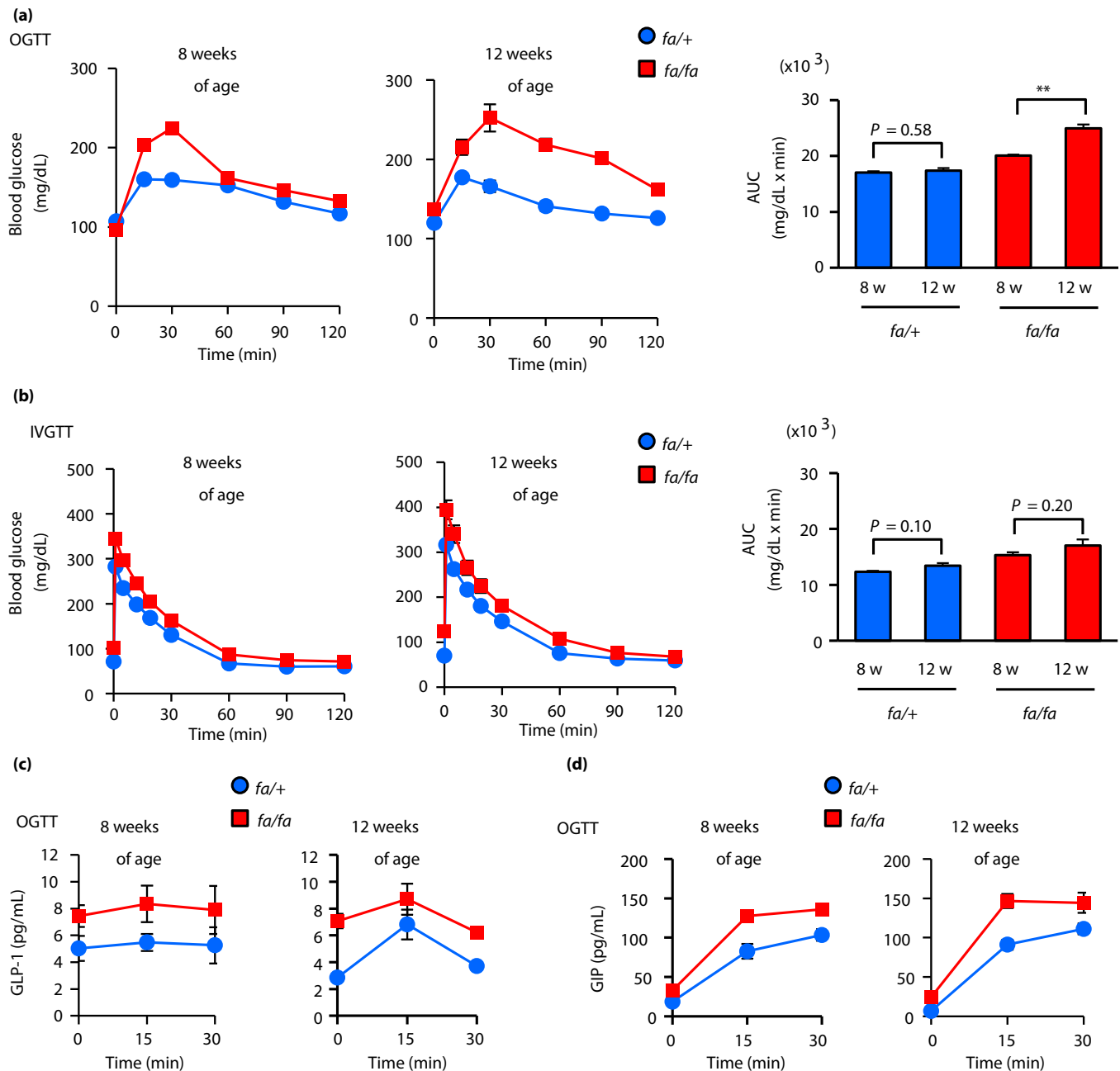


**Figure 1** | Glucose tolerance to oral, but not intravenous, load deteriorates with age in Zucker fatty diabetes mellitus (ZFDM) *fa/fa* rats. (a,b) Glucose tolerance tests of ZFDM rats. (a) Oral glucose tolerance test (OGTT) and (b) intravenous glucose tolerance test were carried out on ZFDM rats ( $n = 5-6$ ). Right: blood glucose levels; left: area under the curve (AUC) of the levels. The data are expressed as the mean  $\pm$  standard error of the mean. Holm's method was used for evaluation of statistical significance. \*\* $P < 0.01$ . (c) Plasma glucagon-like peptide 1 (GLP-1) and (d) glucose-dependent insulinotropic polypeptide (GIP) levels during OGTT.

control *fa/+* rats, even at 12 weeks-of-age (Figure 2d). These results suggest that ZFDM *fa/fa* rats at 12 weeks-of-age are useful for investigating the mechanisms underlying functional differences between non-large islets and enlarged islets in the same animal model.

#### Enlarged islets of ZFDM *fa/fa* rats show diminished incretin-induced insulin secretion

We next examined insulin content and insulin secretion from isolated islets of ZFDM rats at 8 and 12 weeks-of-age. At 8 weeks-of-age, although basal insulin secretion was relatively

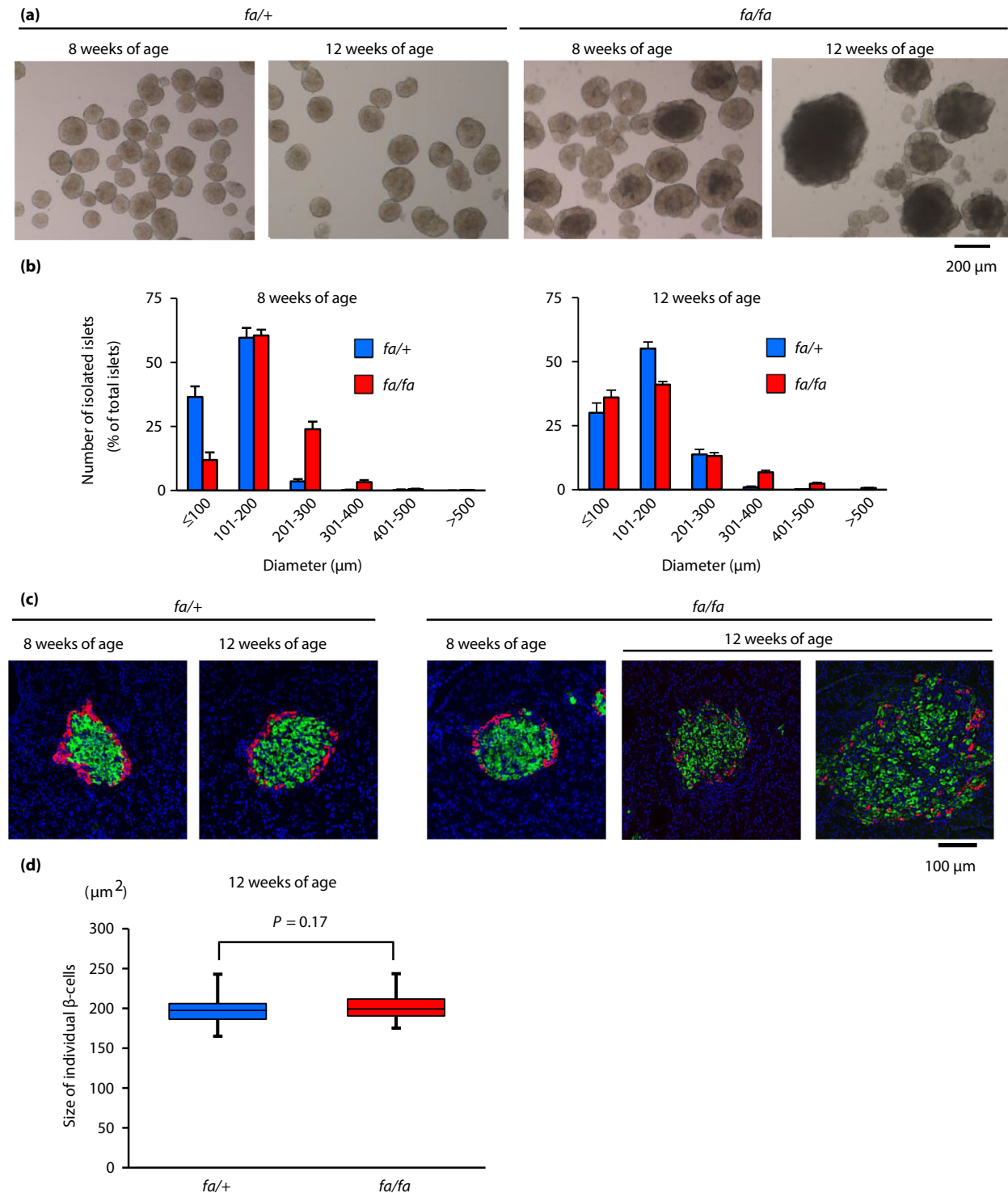


**Figure 2** | Pancreata of Zucker fatty diabetes mellitus (ZFDM) *fa/fa* rats contain both non-large islets and enlarged islets. (a) Microscopic image of isolated pancreatic islets of ZFDM rats. Several islets, especially the enlarged islets, are thick and appear black due to poor light transmission. (b) Size distribution of isolated islets of ZFDM rats. Diameters of 200–700 islets of each rat were measured with microscopy ( $n = 8$  for *fa/+* rats;  $n = 6$  for *fa/fa* rats). (c) Immunostaining of pancreata of ZFDM rats. Green, insulin; red, glucagon; blue, 4',6-diamidino-2-phenylindole. ZFDM rats at 12 weeks-of-age had pancreatic islets of various sizes. (d) Size of individual  $\beta$ -cells in the islets of ZFDM rats. The data are presented by box-and-whisker plots of 50 islets for each genotype. Welch's *t*-test was used for evaluation of statistical significance.

high in the islets of *fa/fa* rats, both GIIS and IIIS were retained (Figure 3a, Figure S3a). At 12 weeks-of-age, GIIS in both non-large islets and enlarged islets was retained to some extent. IIIS in the non-large islets of the *fa/fa* rats was reduced, but not significantly, compared with that in the *fa/+* islets, whereas IIIS was significantly diminished in the enlarged islets (Figure 3b, Figures S3b,S4). Insulin content standardized by deoxyribonucleic acid content was decreased in both non-large and enlarged islets of ZFDM rats at 12 weeks-of-age (Figure S3b), which is not comparable to the human study using islets of non-diabetic donors<sup>23</sup>. As IIIS in the enlarged islets was significantly reduced compared with that in the non-large islets of ZFDM rats at 12 weeks-of-age while there were no differences in the expression levels of the incretin receptors (*Glp1r* and *Gipr*) between the enlarged and non-large islets of these rats (Figure 3c,d), the blunted insulin response to the incretins cannot be explained only by the reduced expressions of the incretin receptors.

#### Gene expression profile of the enlarged islets of ZFDM *fa/fa* rats is similar to that of undifferentiated, proliferative cells

To clarify the mechanism underlying impaired incretin responsiveness in the enlarged islets of *fa/fa* rats, we carried out RNA sequencing-based transcriptome analysis of these islets. Expressions of the genes related to  $\beta$ -cell differentiation, including *Pdx1*, *Nkx6-1*, *Neurod1* and *Mafa*, were markedly decreased in the enlarged islets of *fa/fa* rats, compared with those in non-large islets (Figure 4). In contrast, expression of the genes related to cell proliferation, such as *Mki67* (Ki67), *Myc* and *Mcm2* (deoxyribonucleic acid replication licensing factor), were significantly increased or tended to be increased. *Hif1a*, which is induced by hypoxia, tended to be increased in the enlarged islets of *fa/fa* rats. The changes in gene expressions were further confirmed at protein levels by immunostaining of pancreata for *Pdx1*, *Myc* and Ki67 (Figure S5). Expressions of genes encoding the islet hormones *Ins1* (insulin 1), *Ins2* (insulin 2), *Gcg* (glucagon) and *Sst* (somatostatin) in the enlarged islets of *fa/fa* rats were significantly decreased or tended to be decreased compared with those in non-large islets (Figure 4). Furthermore, expressions of the genes required for  $\beta$ -cell function, such as *Abcc8* (Sur1), *Kcnj11* (Kir6.2), *Cacna1d* (Cav1.3) and *Pcsk1* (PC1/3), were significantly decreased compared with those in non-large islets (Figure 4). These results showed that the identity of the  $\beta$ -cells is lost in *fa/fa* rats, especially in the enlarged islets, and that the gene expression profile of the enlarged islets is similar to that of undifferentiated, proliferative cells.

We have also found that the expression of *Aldh1a3*, which is now known to be a dedifferentiation marker, was increased in the enlarged islets, whereas that of *Chga*, a general endocrine marker, was reduced in the enlarged islets. The endocrine progenitor marker, *Neurog3* (*Ngn3*), was not expressed in the enlarged islets, and the  $\alpha$ -cell markers, *Arx* and *Pou3f4* (*Brn4*), were not increased in the enlarged islets. These findings suggest that  $\beta$ -cells in the enlarged islets were dedifferentiated to the

state of endocrine precursor or immature  $\beta$ -cells, and were not transdifferentiated to  $\alpha$ -cells.

Pathway analysis of differentially expressed genes among islets of *fa/+* and *fa/fa* rats at 12 weeks-of-age suggested that genes related to maturity onset of diabetes of the young, insulin secretion and type 2 diabetes are highly enriched (Table S1).

#### Enlarged islets of ZFDM *fa/fa* rats show glucose metabolism characteristic of tumor cells

As the enlarged islets of the *fa/fa* rats showed a gene expression profile characteristic of undifferentiated, proliferative cells, we reasoned that glucose metabolism might be changed in the enlarged islets. To address this, we examined glucose metabolism by using transcriptomic and metabolomic approaches (Figure 5a,b). Interestingly, the expressions of *Slc2a2* (Glut2), a major glucose transporter in rodent  $\beta$ -cells, and *Gck* (glucokinase), the first rate-limiting enzyme in glucose metabolism and the glucose sensor in  $\beta$ -cells, were markedly decreased in the enlarged islets of *fa/fa* rats compared with those in non-large islets, whereas expressions of *Slc2a1* (Glut1), a major glucose transporter in tumor cells<sup>24</sup>, and *Hk2* (hexokinase 2), a major hexokinase in tumor cells<sup>25</sup>, were increased in the enlarged islets, suggesting an increased sensitivity to glucose. In addition, the expressions of *Gpi* (glucose-6-phosphate isomerase), *Pfkfb* (phosphofructokinase), the rate-limiting enzyme of glycolysis and *Pgk1* (phosphoglycerate kinase) were increased or tended to be increased in the enlarged islets compared with those in the non-large islets. An increase in fructose 6-phosphate content by glucose stimulation further supported enhanced glycolysis in the enlarged islets (Figure 5c).

#### Pyruvate produced in glycolysis serves as a substrate for the tricarboxylic acid cycle or lactate production

In the enlarged islets, the expression of *Ldha* (lactate dehydrogenase), which converts pyruvate to lactate, was increased, whereas the expression of *Pdhb* (pyruvate dehydrogenase), which catalyzes the oxidative decarboxylation of pyruvate to produce acetyl coenzyme A, was decreased significantly (Figure 5a,b). The expression of *Pdk1* (pyruvate dehydrogenase kinase), which inactivates Pdh, was significantly increased in the enlarged islets. In addition, the expression of *Slc16a3* (Mct4, monocarboxylate transporter), which exports lactate from cells, was markedly increased in the enlarged islets. Measurement of lactate in the islet culture media showed that lactate production was indeed increased in the enlarged islets (Figure 5d). These results together show that glucose metabolism of the enlarged islets of *fa/fa* rats resembles that of tumor cells.

#### Enlarged islets of ZFDM *fa/fa* rats show abnormalities in mitochondrial function and morphology

It is well known that tumor cells produce adenosine triphosphate mainly through a high rate of glycolysis rather than mitochondrial oxidative phosphorylation, even in aerobic conditions, a phenomenon called the "Warburg effect"<sup>26</sup>. We



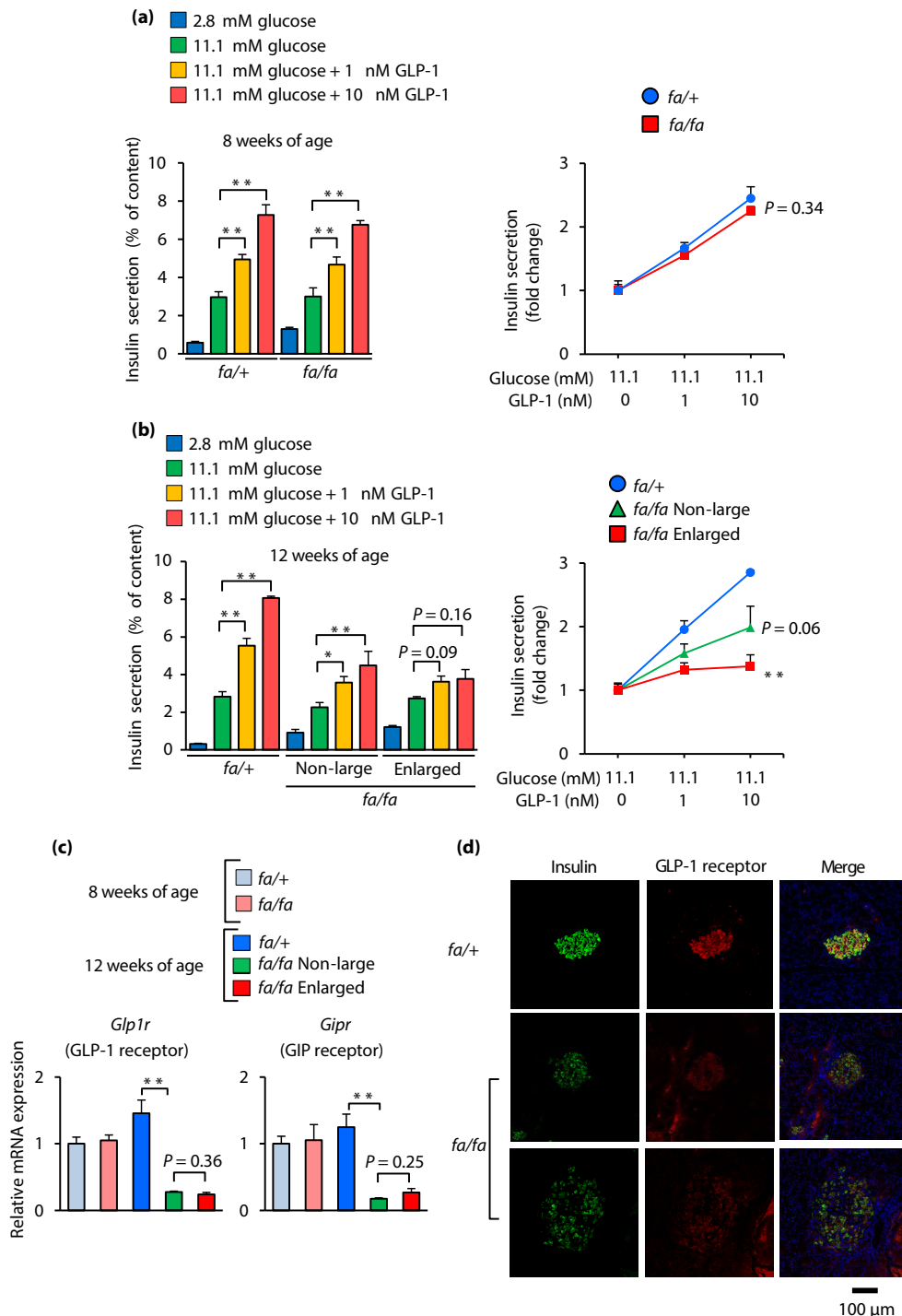


**Figure 3** | The enlarged islets of Zucker fatty diabetes mellitus (ZFDM) *fa/fa* rats show diminished incretin-induced insulin secretion. (a,b) Insulin secretion from isolated islets of ZFDM rats at (a) 8 and (b) 12 weeks-of-age. The islets were stimulated with glucose and glucagon-like peptide 1 (GLP-1; *n* = 5–8). Insulin secretion was normalized by cellular insulin content (left) and presented as fold-change relative to the amount of insulin secretion at 11.1 mmol/L glucose (right). The data are expressed as the mean  $\pm$  standard error of the mean. Holm's method was used for evaluation of statistical significance versus 11.1 mmol/L glucose (left) or versus *fa/+* (right). \**P* < 0.05; \*\**P* < 0.01. (c) Expression levels of genes encoding incretin receptors. Messenger ribonucleic acid expression levels are presented as fold-change relative to those of *fa/+* rats at 8 weeks of age (*n* = 3). The data are expressed as the mean  $\pm$  standard error of the mean. Holm's method was used for evaluation of statistical significance. \*\**P* < 0.01. (d) Immunostaining of pancreata of ZFDM rats at 12 weeks-of-age. Green, insulin; red, GLP-1 receptor; Blue, 4',6-diamidino-2-phenylindole.



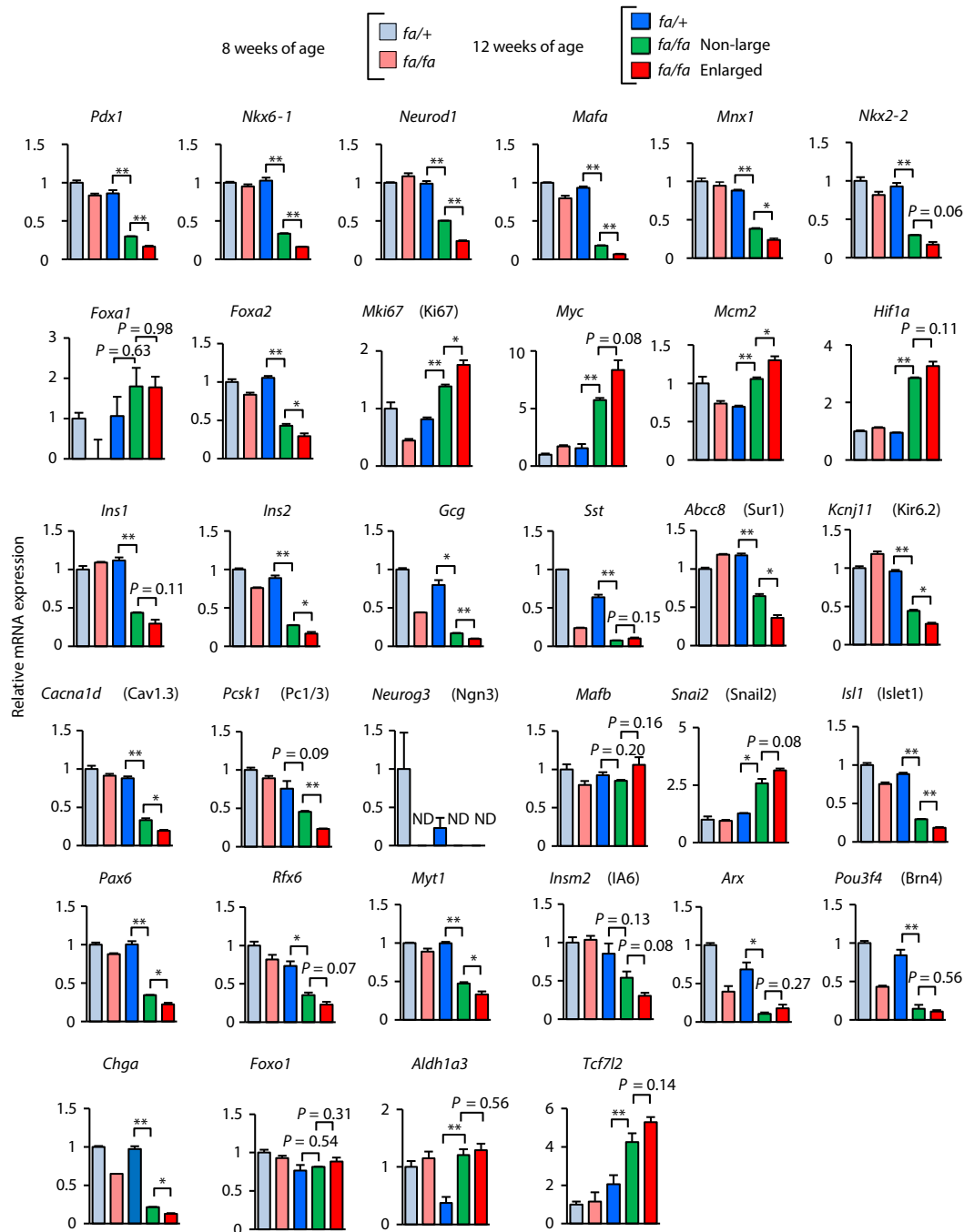


**Figure 4** | The gene expression profile of the enlarged islets is similar to that of undifferentiated, proliferative cells. Expression levels of genes related to  $\beta$ -cell differentiation, proliferation, dedifferentiation and genes encoding islet hormones. Messenger ribonucleic acid (mRNA) expression levels are presented as fold-change relative to those of *fa/+* rats at 8 weeks-of-age ( $n = 3$ ). The data are expressed as means  $\pm$  standard error of the mean. Holm's method was used for evaluation of statistical significance. \* $P < 0.05$ ; \*\* $P < 0.01$ . *Pdx1*, pancreatic and duodenal homeobox 1; *Nkx6-1*, NK6 homeobox 1; *Neurod1*, neuronal differentiation 1; *MafA*, MAF bZIP transcription factor A; *Mnx1*, motor neuron and pancreas homeobox 1; *Nkx2-2*, NK2 homeobox 2; *Foxa1*, forkhead box A1; *Foxa2*, forkhead box A2; *Mki67*, marker of proliferation Ki-67; *Myc*, MYC proto-oncogene, bHLH transcription factor; *Mcm2*, minichromosome maintenance complex component 2; *Hif1a*, hypoxia inducible factor 1 subunit alpha; *Ins1*, insulin 1; *Ins2*, insulin 2; *Gcg*, glucagon; *Sst*, somatostatin; *Abcc8*, ATP binding cassette subfamily C member 8; *Kcnj11*, potassium inwardly-rectifying channel, subfamily J, member 11; *Cacna1d*, calcium voltage-gated channel subunit alpha1 D; *Pcsk1*, proprotein convertase subtilisin/kexin type 1; *Neurog3*, neurogenin 3; *MafB*, MAF bZIP transcription factor B; *Snai2*, snail family transcriptional repressor 2; *Isl1*, ISL LIM homeobox 1; *Pax6*, paired box 6; *Rfx6*, regulatory factor X, 6; *Myt1*, myelin transcription factor 1; *Insm2*, INSM transcriptional repressor 2; *Arx*, aristaless related homeobox; *Pou3f4*, POU class 3 homeobox 4; *Chga*, chromogranin A; *Foxo1*, forkhead box O1; *Aldh1a3*, aldehyde dehydrogenase 1 family, member A3; *Tcf7l2*, transcription factor 7 like 2; ND, not detected.

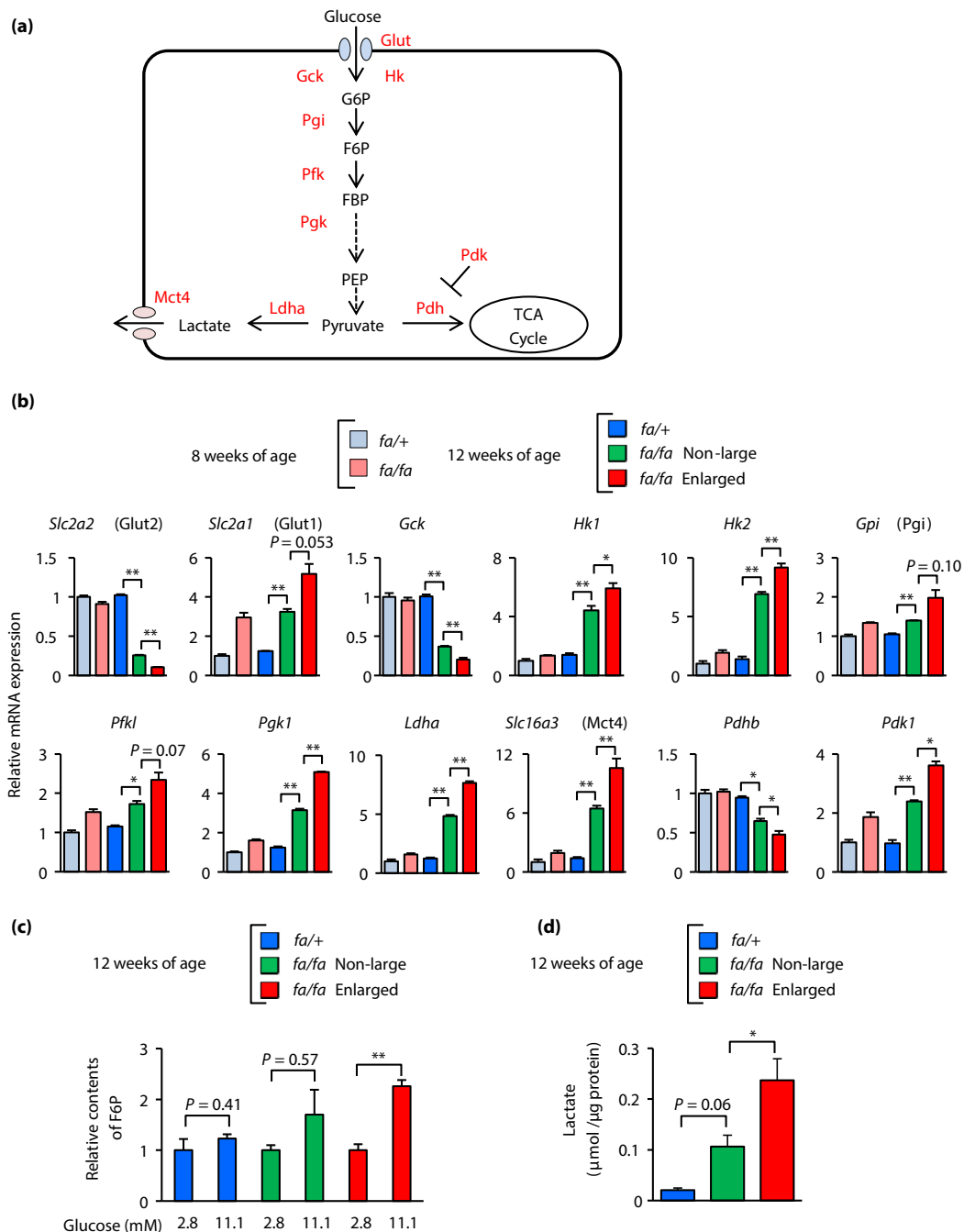


**Figure 5** | The enlarged islets show glucose metabolism characteristic of tumor cells. (a) A schematic view of the glycolysis and lactate production pathways. Metabolites are shown in black; proteins are shown in red. (b) Expression levels of genes associated with glycolysis and lactate production. Messenger ribonucleic acid (mRNA) expression levels are presented as fold-change relative to those of *fa/+* rats at 8 weeks-of-age ( $n = 3$ ). The data are expressed as the mean  $\pm$  standard error of the mean. Holm's method was used for evaluation of statistical significance. \* $P < 0.05$ ; \*\* $P < 0.01$ . (c) Cellular contents of fructose 6-phosphate (F6P). The contents of F6P are presented as fold-change relative to those under low glucose (2.8 mmol/L) condition ( $n = 3$ ). The data are expressed as the mean  $\pm$  standard error of the mean. Holm's method was used for evaluation of statistical significance. \*\* $P < 0.01$ . (d) Lactate production. The amount of lactate in culture media was corrected by the amount of protein in the pancreatic islets used for the culture ( $n = 3-6$ ). The data are expressed as the mean  $\pm$  standard error of the mean. Holm's method was used for evaluation of statistical significance. \* $P < 0.05$ . *Slc2a2*, solute carrier family 2 member 2; *Slc2a1*, solute carrier family 2 member 1; *Gck*, glucokinase; *Hk1*, hexokinase 1; *Hk2*, hexokinase 2; *Gpi*, glucose-6-phosphate isomerase; *Pfk1*, phosphofructokinase, liver type; *Pgk1*, phosphoglycerate kinase 1; *Ldha*, lactate dehydrogenase A; *Slc16a3*, solute carrier family 16 member 3; *Pdhb*, pyruvate dehydrogenase E1 subunit beta; *Pdk1*, pyruvate dehydrogenase kinase 1.

therefore examined the tricarboxylic acid (TCA) cycle-associated genes and metabolites, and found that expression of *Fh* was significantly decreased in the enlarged islets of *fal/fa* rats, and also that *Aco2* and *Suc1g1* (Succinate-CoA ligase) tended to be decreased in the enlarged islets (Figure 6a,b). Consistently, productions by glucose of fumarate and malate, the metabolites in the TCA cycle, were decreased (Figure 6c).

The MA shuttle couples with both glycolysis and the TCA cycle, through which cellular glutamate, a key signal for IIS, is produced<sup>5</sup>. We then examined the gene expressions and metabolites associated with the MA shuttle. Although changes in the expressions of *Got1*, *Got2* and *Mdh2* were not obvious in the enlarged islets, as compared with those of the non-large islets, expression of *Mdh1* in the enlarged islets was significantly reduced (Figure 6a,b). It was noteworthy that production by glucose of cellular glutamate was diminished in the enlarged islets (Figure 6c). These results suggest mitochondrial dysfunction in the enlarged islets. We therefore carried out morphological examination of mitochondria by transmission electron microscopy. We observed swollen and ruptured mitochondria in  $\beta$ -cells of *fal/fa* rats (Figure S6). As the majority of mitochondria in  $\beta$ -cells of *fa/+* rats showed  $<0.3\ \mu\text{m}$  in the short diameter (Figure S6), we defined swollen mitochondria as those having short diameter  $>0.3\ \mu\text{m}$ . The number of swollen mitochondria was significantly increased in the enlarged islets (Figure 6d). In addition, the number of ruptured mitochondria, which had a truncated outer membrane and matrix density similar to cytoplasm, was markedly increased in the enlarged islets (Figure 6d). Furthermore, we examined mitochondrial oxidative phosphorylation directly by measuring the OCR. Glucose (12 mmol/L)-stimulated OCR was markedly reduced in the enlarged islets (Figure 6e, Figure S7). These results indicate morphological and functional abnormalities in the  $\beta$ -cell mitochondria of the enlarged islets.

## DISCUSSION

Although studies of various animal models and humans have shown that pancreatic islets are morphologically and functionally heterogeneous, the relationship between incretin responsiveness and islet heterogeneity is not known, nor is the mechanism underlying incretin unresponsiveness in  $\beta$ -cells in obese type 2 diabetes. To address this issue, we have characterized the non-large islets ( $\leq 200\ \mu\text{m}$  in diameter) and the enlarged islets ( $>300\ \mu\text{m}$  in diameter) of ZFDM *fal/fa* rats separately, and compared their functional properties. We found an age-dependent increase in the number of enlarged islets in the *fal/fa* rats. Mildly enlarged islets ( $>200\ \mu\text{m}$  in diameter) already appeared at 8 weeks-of-age, and a small portion of islets showed greater enlargement ( $>300\ \mu\text{m}$  in diameter) at the same weeks of age (Figure 2, Figure S1). In addition, transcriptome analysis suggested that enhancement of glycolysis began to occur between 8 and 12 weeks-of-age. Thus, it is likely that islets of ZFDM *fal/fa* rats begin to become enlarged between 8 and 12 weeks-of-age, and that the number of enlarged islets

increases with age. There are two possibilities for the enlargement of pancreatic islets: (i) the size of individual  $\beta$ -cells becomes enlarged; or (ii) the number of  $\beta$ -cells is increased<sup>27</sup>. Individual  $\beta$ -cell size of *fal/fa* rats was similar to that of control *fa/+* rats, even at 12 weeks-of-age (Figure 2d), indicating that the number of pancreatic  $\beta$ -cells was increased in the enlarged islets. A similar result has been reported in a human study in which  $\beta$ -cell mass was increased by  $\sim 50\%$  in obese individuals compared with normal individuals, whereas there was no increase in individual  $\beta$ -cell size<sup>28</sup>.

We found in the present study that the expression levels of the genes for  $\beta$ -cell differentiation including, *Nkx6-1* and *Mafa*, which were reported as maturation markers<sup>29–31</sup>, were decreased in the enlarged islets, whereas those for cell proliferation were increased, suggesting that the phenotype of enlarged islets resembles that of undifferentiated, proliferative cells. Recent studies using a method for  $\beta$ -cell tracing have shown that  $\beta$ -cells can be dedifferentiated under certain conditions *in vitro*<sup>32</sup> and *in vivo*, such as in type 2 diabetes<sup>33</sup>. Our findings in the enlarged islets that the dedifferentiation marker *Aldh1a3* was increased while the endocrine progenitor marker *Neurog3* (Ngn3) was not expressed and that the  $\alpha$ -cell markers *Arx* and *Pou3f4* (Brn4) were not increased suggest that  $\beta$ -cells in the enlarged islets were dedifferentiated to the state of endocrine precursor or immature  $\beta$ -cells, and were not transdifferentiated to  $\alpha$ -cells (Figure 4). In addition, the islets of the *fal/fa* rats began to be destroyed after 12 weeks-of-age<sup>13,14</sup>. Thus, both  $\beta$ -cell dedifferentiation and islet fragility might cause  $\beta$ -cell failure, resulting in the development of type 2 diabetes in the *fal/fa* rats. The transcription factor, *Tcf7l2*, is known to be involved in the regulation of the expressions of incretin receptors and insulin<sup>34,35</sup>. Gene expression of *Tcf7l2* was reported to be increased in islets of obese diabetic mice, but the protein level of *Tcf7l2* was rather decreased. The protein levels of human TCF7L2, GLP1R and GIPR were also found to be decreased in islets from patients with type 2 diabetes<sup>34</sup>. We showed that gene expression of *Tcf7l2* was increased in both non-large and enlarged islets of *fal/fa* rats (Figure 4). However, similar to the findings mentioned above, the protein level of *Tcf7l2* might be decreased in both non-large and enlarged islets.

Glucose metabolism in tumor cells has been extensively studied in recent years<sup>24,36,37</sup>. It is well known that tumor cells show enhanced glucose uptake and glycolysis, and that much of the pyruvate produced by glycolysis is converted to lactate rather than undergoing mitochondrial oxidation through the TCA cycle<sup>38,39</sup>. This phenomenon occurs even under aerobic conditions (aerobic glycolysis) and is called the “Warburg effect”<sup>26</sup>. Our transcriptome and metabolome data show that aerobic glycolysis occurs especially in the enlarged islets of *fal/fa* rats. Decreased OCR has also been shown to occur in tumor cells<sup>40–42</sup>. Indeed, the enlarged islets of *fal/fa* rats showed decreased OCR, which is indicative of mitochondrial dysfunction. The effect of hypoxia in the enlarged islets during 3-day culture is limited, as the expression of *Hif1a* is already

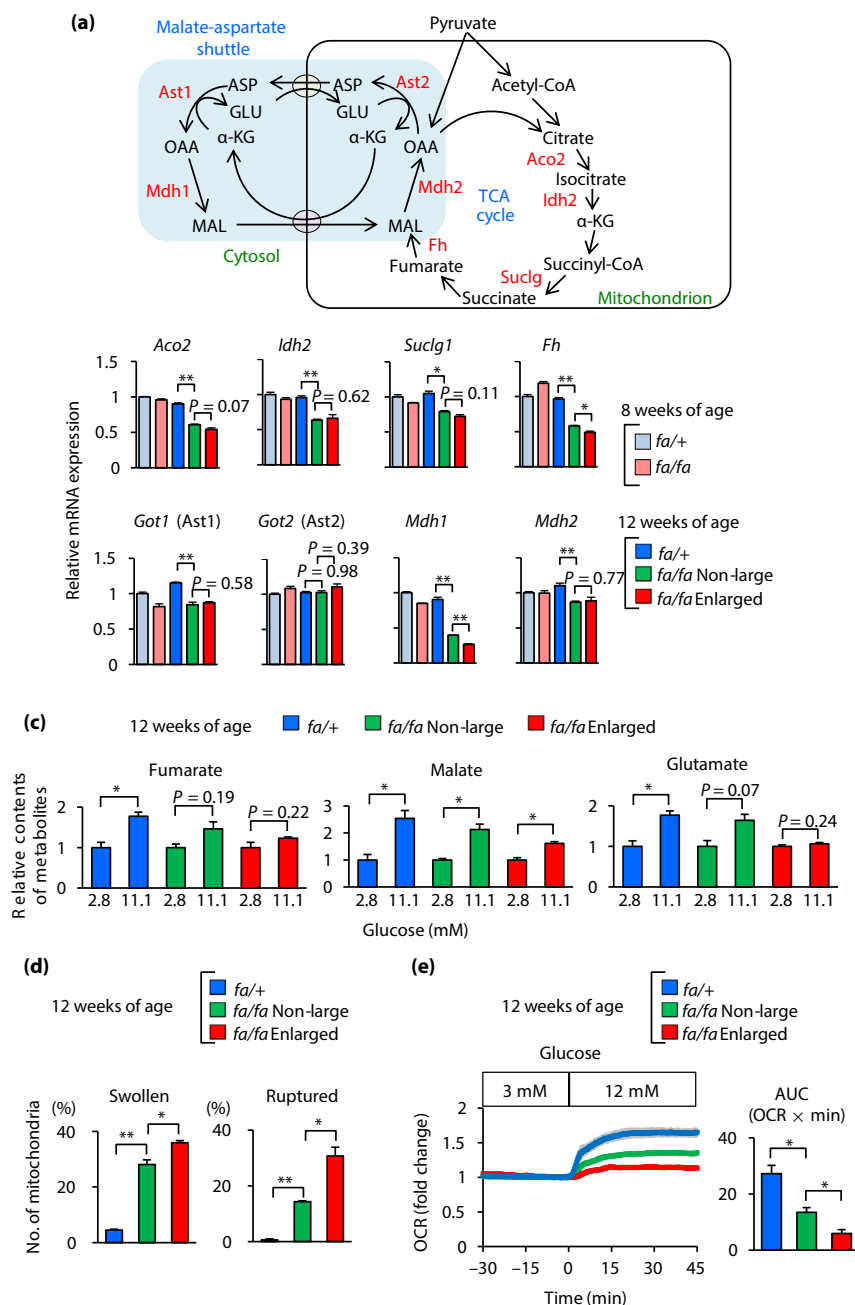


**Figure 6** | The enlarged islets show abnormalities in mitochondrial morphology and function. (a) A schematic view of the tricarboxylic acid (TCA) cycle and malate-aspartate (MA) shuttle. Metabolites are shown in black; and proteins are shown in red. (b) Expression levels of genes associated with the TCA cycle and MA shuttle. Messenger ribonucleic acid (mRNA) expression levels are presented as fold-change relative to those of *fa/+* rats at 8 weeks-of-age ( $n = 3$ ). The data are expressed as the mean  $\pm$  standard error of the mean. Holm's method was used for evaluation of statistical significance.  $*P < 0.05$ ;  $**P < 0.01$ . (c) Metabolites associated with the TCA cycle and MA shuttle. Contents of metabolites are presented as fold-change relative to those under low glucose (2.8 mmol/L) condition ( $n = 3$ ). The data are expressed as the mean  $\pm$  standard error of the mean. Holm's method was used for evaluation of statistical significance.  $*P < 0.05$ . (d) The percentages of swollen and ruptured mitochondria ( $n = 3$  each). The data are expressed as the mean  $\pm$  standard error of the mean. Holm's method was used for evaluation of statistical significance.  $*P < 0.05$ ;  $**P < 0.01$ . (e) The oxygen consumption rate (OCR) of Zucker fatty diabetes mellitus islets. The OCR values obtained under high-glucose (12 mmol/L) condition are presented as fold-change relative to those under low-glucose (3 mmol/L) condition (left), and are also presented as the area under the curve (AUC) during high-glucose stimulation (right;  $n = 3$ –4). The data are expressed as the mean  $\pm$  standard error of the mean. Holm's method was used for evaluation of statistical significance.  $*P < 0.05$ . Aco2, aconitase 2; Idh2, isocitrate dehydrogenase (NADP(+)) 2; Succlg1, succinate-CoA ligase GDP/ADP-forming subunit alpha; Fh, fumarate hydratase; Got1, glutamic-oxaloacetic transaminase 1; Got2, glutamic-oxaloacetic transaminase 2; Mdh1, malate dehydrogenase 1; Mdh2, malate dehydrogenase 2.

increased in the *fa/fa* non-large islets, the size of which is comparable to that of the islets of *fa/+* rats (Figure 4). We also found that in  $\beta$ -cells of the enlarged islets, ~40% of mitochondria showed a swollen shape, and a significant number of the mitochondria showed ruptured membranes. This type of mitochondrial abnormality was reported in tumor cells<sup>43</sup> and diabetic islets<sup>44,45</sup>.

We found that insulin secretion at a low concentration of glucose (2.8 mmol/L glucose) tended to be increased in the enlarged islets (Figure S4). The gene expression data shown in Figure 5 showed that Glut1, which has lower  $V_{max}$  than Glut2, was increased in the enlarged islets compared with non-large islets, and that Hk1 and Hk2, both of which have higher affinity to glucose than Gck, were increased in the enlarged islets. These findings could account for increased glucose sensitivity in the enlarged islets. We recently reported that glutamate produced from glucose through the MA shuttle is a key signal in IIIS<sup>5</sup>, and that  $\beta$ -cell lines deficient for AST1, a critical enzyme in cytosolic glutamate production through the MA shuttle, showed impaired IIIS<sup>6</sup>. We showed here that IIIS is diminished in the enlarged islets, and that this is accompanied by decreased glutamate production. These findings further support the notion that impaired incretin responsiveness is well correlated with impaired glutamate production in the pancreatic islets<sup>5</sup>.

These findings together show that glucose metabolism of enlarged islets of ZFDM rats resembles that of tumor cells. Dedifferentiation of islets cells might well induce such metabolic changes, resulting in various abnormalities in  $\beta$ -cell functions. As the number of enlarged islets is increased with age in ZFDM *fa/fa* rats, it is of interest to investigate the relationship between aging and the development of tumor-like metabolic features in enlarged islets.

The enlarged islets of ZFDM *fa/fa* rats and tumor cells possess common features in gene expression profile and glucose metabolism. This phenotype might well underlie incretin unresponsiveness and  $\beta$ -cell failure in diabetes; our data might provide new insight into the relationship between size and function of diabetic human islets. Although it will be necessary to study functional differences between non-large and enlarged islets in different animal models of diabetes, elucidation of the mechanisms underlying  $\beta$ -cell failure in the enlarged islets of ZFDM rats might provide the basis for the development of novel drugs for treatment of the disease, as well as better understanding of the pathogenesis and pathophysiology of diabetes.

## ACKNOWLEDGMENTS

We thank Graeme Bell, Christopher M Carmean, Ghupurjan Ghani, Mahira Hashim and Yutaka Seino for valuable comments and suggestions; Kanako Tamura, Ritsuko Hoshikawa, Shihomi Hidaka, Ayako Kawabata and Chihiro Seki for their excellent technical assistance; and Grace K Honkawa for editing the manuscript. We are grateful to MSD K.K., Novo Nordisk Pharma Ltd., Kowa Pharmaceutical Co., Ltd., and Taisho

Pharmaceutical Co., Ltd. for their generous supports. This study was supported by AMED under Grant Number JP19gm5010002 (S.S.) and JP19gm5010003 (S.S.); JSPS KAKENHI JP18H02364 (N.Y.); the Kobayashi Foundation; and the Cell Function Analysis Core of the University of Washington Diabetes Research Center (NIH grant number P30 DK017047) (I.S.).

## DISCLOSURE

The authors declare no conflict of interest.

## REFERENCES

- Drucker DJ. Incretin action in the pancreas: potential promise, possible perils, and pathological pitfalls. *Diabetes* 2013; 62: 3316–3323.
- Nauck M, Stöckmann F, Ebert R, *et al.* Reduced incretin effect in Type 2 (non-insulin-dependent) diabetes. *Diabetologia* 1986; 29: 46–52.
- Bando Y, Kanehara H, Aoki K, *et al.* Obesity may attenuate the HbA1c-lowering effect of sitagliptin in Japanese type 2 diabetic patients: Obesity may attenuate sitagliptin's effects. *J Diabetes Investig* 2012; 3: 170–174.
- Cho YM. Incretin physiology and pathophysiology from an Asian perspective. *J Diabetes Investig* 2015; 6: 495–507.
- Gheni G, Ogura M, Iwasaki M, *et al.* Glutamate acts as a key signal linking glucose metabolism to incretin/cAMP action to amplify insulin secretion. *Cell Rep* 2014; 9: 661–673.
- Murao N, Yokoi N, Honda K, *et al.* Essential roles of aspartate aminotransferase 1 and vesicular glutamate transporters in  $\beta$ -cell glutamate signaling for incretin-induced insulin secretion. *PLoS ONE* 2017; 12: e0187213.
- Singh SP, Janjuha S, Hartmann T, *et al.* Different developmental histories of beta-cells generate functional and proliferative heterogeneity during islet growth. *Nat Commun* 2017; 8: 664.
- Benninger RKP, Hodson DJ. New understanding of  $\beta$ -cell heterogeneity and in situ islet function. *Diabetes* 2018; 67: 537–547.
- Chan CB, Wright GM, Wadowska DW, *et al.* Ultrastructural and secretory heterogeneity of *fa/fa* (Zucker) rat islets. *Mol Cell Endocrinol* 1998; 136: 119–129.
- MacGregor RR, Williams SJ, Tong PY, *et al.* Small rat islets are superior to large islets in in vitro function and in transplantation outcomes. *Am J Physiol Endocrinol Metab* 2006; 290: E771–E779.
- Farhat B, Almelkar A, Ramachandran K, *et al.* Small human islets comprised of more  $\beta$ -cells with higher insulin content than large islets. *Islets* 2013; 5: 87–94.
- Kilimnik G, Zhao B, Jo J, *et al.* Altered islet composition and disproportionate loss of large islets in patients with type 2 diabetes. *PLoS ONE* 2011; 6: e27445.
- Yokoi N, Hoshino M, Hidaka S, *et al.* A novel rat model of type 2 diabetes: the Zucker fatty diabetes mellitus ZFDM rat. *J Diabetes Res* 2013; 2013: 1–9.

14. Gheni G, Yokoi N, Beppu M, *et al.* Characterization of the prediabetic state in a novel rat model of type 2 diabetes, the ZFDM rat. *Journal of Diabetes Research* 2015; 1–8.
15. Yokoi N, Beppu M, Yoshida E, *et al.* Identification of putative biomarkers for prediabetes by metabolome analysis of rat models of type 2 diabetes. *Metabolomics* 2015; 11: 1277–1286.
16. Okeda T, Ono J, Takaki R, *et al.* Simple method for the collection of pancreatic islets by the use of Ficoll-Conray gradient. *Endocrinologia Japonica* 1979; 26: 495–499.
17. Carter JD, Dula SB, Corbin KL, *et al.* A practical guide to rodent islet isolation and assessment. *Biol Proc Online* 2009; 11: 3–31.
18. Tamura K, Minami K, Kudo M, *et al.* Liraglutide improves pancreatic beta cell mass and function in alloxan-induced diabetic mice. *PLoS ONE* 2015; 10: e0126003.
19. Huang DW, Sherman BT, Lempicki RA. Systematic and integrative analysis of large gene lists using DAVID Bioinformatics Resources. *Nat Protoc* 2009; 4: 44–57.
20. Huang DW, Sherman BT, Lempicki RA. Bioinformatics enrichment tools: paths toward the comprehensive functional analysis of large gene lists. *Nucleic Acids Res* 2009; 37: 1–13.
21. Mizoguchi A, Nakanishi H, Kimura K, *et al.* Nectin: an adhesion molecule involved in formation of synapses. *J Cell Biol* 2002; 156: 555–565.
22. Jung S-R, Reed BJ, Sweet IR. A highly energetic process couples calcium influx through L-type calcium channels to insulin secretion in pancreatic  $\beta$ -cells. *Am J Physiol Endocrinol Metab* 2009; 297: E717–E727.
23. Farhat B, Almelkar A, Ramachandran K, *et al.* Small human islets comprised of more  $\beta$ -cells with higher insulin content than large islets. *Islets* 5: 87–94.
24. Pavlova NN, Thompson CB. The emerging hallmarks of cancer metabolism. *Cell Metab* 2016; 23: 27–47.
25. Mathupala SP, Ko YH, Pedersen PL. Hexokinase II: Cancer's double-edged sword acting as both facilitator and gatekeeper of malignancy when bound to mitochondria. *Oncogene* 2006; 25: 4777–4786.
26. Warburg O, Wind F, Negelein E. The metabolism of tumors in the body. *J Gen Physiol* 1927; 8: 519–530.
27. Kahn SE, Hull RL, Utzschneider KM. Mechanisms linking obesity to insulin resistance and type 2 diabetes. *Nature* 2006; 444: 840–846.
28. Saisho Y, Butler AE, Manesso E, *et al.*  $\beta$ -Cell mass and turnover in humans: effects of obesity and aging. *Diabetes Care* 2013; 36: 111–117.
29. Sander M, Sussel L, Conners J, *et al.* Homeobox gene Nkx6.1 lies downstream of Nkx2.2 in the major pathway of beta-cell formation in the pancreas. *Development* 2000; 127: 5533–5540.
30. Zhao L, Guo M, Matsuoka T, *et al.* The islet cell-enriched MafA activator is a key regulator of insulin gene transcription. *J Biol Chem* 2005; 280: 11887–11894.
31. Bader E, Migliorini A, Gegg M, *et al.* Identification of proliferative and mature  $\beta$ -cells in the islets of Langerhans. *Nature* 2016; 535: 430–434.
32. Minami K, Miyawaki K, Hara M, *et al.* Tracing phenotypic reversibility of pancreatic  $\beta$ -cells in vitro: phenotypic reversibility of  $\beta$ -cells. *J Diabetes Investig* 2010; 1: 242–251.
33. Talchai C, Xuan S, Lin HV, *et al.* Pancreatic  $\beta$  cell dedifferentiation as a mechanism of diabetic  $\beta$  cell failure. *Cell* 2012; 150: 1223–1234.
34. Shu L, Matveyenko AV, Kerr-Conte J, *et al.* Decreased TCF7L2 protein levels in type 2 diabetes mellitus correlate with downregulation of GIP- and GLP-1 receptors and impaired beta-cell function. *Hum Mol Genet* 2009; 18: 2388–2399.
35. da Silva Xavier G, Mondragon A, Sun G, *et al.* Abnormal glucose tolerance and insulin secretion in pancreas-specific Tcf7l2-null mice. *Diabetologia* 2012; 55: 2667–2676.
36. Cairns RA, Harris IS, Mak TW. Regulation of cancer cell metabolism. *Nat Rev Cancer* 2011; 11: 85–95.
37. Hay N. Reprogramming glucose metabolism in cancer: can it be exploited for cancer therapy? *Nat Rev Cancer* 2016; 16: 635–649.
38. Hsu PP, Sabatini DM. Cancer cell metabolism: Warburg and beyond. *Cell* 2008; 134: 703–707.
39. DeBerardinis RJ, Chandel NS. Fundamentals of cancer metabolism. *Science Advances* 2016; 2: e1600200.
40. Chen Y, Cairns R, Papandreou I, *et al.* Oxygen consumption can regulate the growth of tumors, a new perspective on the Warburg effect. *PLoS ONE* 2009; 4: e7033.
41. Papandreou I, Cairns RA, Fontana L, *et al.* HIF-1 mediates adaptation to hypoxia by actively downregulating mitochondrial oxygen consumption. *Cell Metab* 2006; 3: 187–197.
42. Lu J, Tan M, Cai Q. The Warburg effect in tumor progression: Mitochondrial oxidative metabolism as an anti-metastasis mechanism. *Cancer Lett* 2015; 356: 156–164.
43. Giang A-H, Raymond T, Brookes P, *et al.* Mitochondrial dysfunction and permeability transition in osteosarcoma cells showing the Warburg effect. *J Biol Chem* 2013; 288: 33303–33311.
44. Anello M, Lupi R, Spampinato D, *et al.* Functional and morphological alterations of mitochondria in pancreatic beta cells from type 2 diabetic patients. *Diabetologia* 2005; 48: 282–289.
45. Lu H, Koshkin V, Allister EM, *et al.* Molecular and metabolic evidence for mitochondrial defects associated with  $\beta$ -cell dysfunction in a mouse model of type 2 diabetes. *Diabetes* 2010; 59: 448–459.

## SUPPORTING INFORMATION

Additional supporting information may be found online in the Supporting Information section at the end of the article.

**Table S1** | Pathway analysis of differentially expressed genes among islets of *fa/+* and *fa/fa* rats at 12 weeks-of-age.

**Figure S1** | Size distribution of isolated islets of Zucker fatty diabetes mellitus rats.

**Figure S2** | The area measurements of whole pancreas,  $\alpha$ - and  $\beta$ -cells in Zucker fatty diabetes mellitus rats.

**Figure S3** | Released insulin, insulin content, deoxyribonucleic acid content in the islets of Zucker fatty diabetes mellitus rats.

**Figure S4** | Comparison of insulin secretion among islets of *fa/+* and *fa/fa* rats at 12 weeks-of-age.

**Figure S5** | Immunostaining of pancreas.

**Figure S6** | Morphology of the mitochondria in  $\beta$ -cells of Zucker fatty diabetes mellitus rats.

**Figure S7** | Oxygen consumption rate (OCR) of Zucker fatty diabetes mellitus islets.